FFI-RAPPORT

16/01242

Indoor dispersion of sarin by evaporation from liquid pools

–
Siv G. Aalbergsjø
Thomas Vik

TNO innovation for life

FFI Forsvarets forskningsinstitutt

Indoor dispersion of sarin by evaporation from liquid pools

Siv G. Aalbergsjø
Thomas Vik

Norwegian Defence Research Establishment (FFI) 15 August 2016

Keywords

Sarin
Fordamping
Modellering og simulering
spredning

FFI-rapport
FFI-RAPPORT 16/01242

Prosjektnummer
1392

ISBN
P: 978-82-464-2808-6
E: 978-82-464-2809-3

Approved by
Hanne Breivik, *Research Manager*
Magnus Vartdal, *Kompetanseansvarlig - beregningsorientert mekanikk*
Janet Blatny, *Director*

Summary

The threat of terrorist actions involving toxic chemicals is present in today's society, and there is therefore a need for appropriate emergency response planning. An accurate description of the release and dispersion of toxic substances, and the resulting health effects for exposed individuals, is an important element for conducting emergency planning.

Norway and the Netherlands started in 2015 a collaborative effort named "The Strategic Mutual Assistance in Research & Technology (SMART) on CBRN Protection". There are several projects within this collaboration. One of them is "CBRN Modelling & Simulation", which aims to combine the CBRN modelling and simulation capabilities in the two nations into an improved capability for mutual benefit. This report describes work performed within the "SMART-CBRN Modelling & Simulation" project.

A terror scenario with dispersion of sarin inside a convention centre is investigated and described in this report. The dispersion of sarin vapour through the convention centre is simulated with the use of two different computational fluid dynamics approaches, large eddy simulations and Reynolds-averaged Navier-Stokes simulations, which have different degrees of accuracy and computational effort. Evaporation from liquid pools at two different locations are calculated separately with an analytical model which depends on the simulated air flow field. From the resulting concentration fields, the impact on humans present in the convention centre is investigated based on the onset of various symptoms.

Our studies show that the evaporation rate depends on the location of the liquid pools. Near the pools, mild impacts on humans like impaired vision set in within a few minutes, while severe impacts or death do not occur until more than half an hour after the evaporation starts. The simulations show that the vapour is not transported very efficiently away from the source. For pool 1, which is in a semi-confined room, hazardous levels of vapour in the neighbouring rooms are not reached until 10–30 minutes after start of the release. For pool 2, which is in the hallway outside the rooms, very little vapour enters the rooms. The presence and movement of people are disregarded in the simulations, as these are computationally difficut to include. In reality this would lead to a more efficient mixing of vapour and air and provide a different dispersion pattern of the vapour. There are also evacuation gates from the halls to the outside, and which remain closed in the simulations; the air velocity field will be affected if these gates are opened.

Large eddy simulations provide larger fluctuations in the velocity fields, and will likely give a more realistic simulation of the vapour transport through the centre, than the Reynolds-averaged Navier-Stokes simulations.

The results from the simulations can be used as reference to evaluate the accuracy of other simpler and faster models, for instance the indoor dispersion models G-COMIS or CONTAM, as well as for conducting exercises and for emergency planning. A useful continuation of the work at hand would be to conduct experiments in order to validate the computational models.

Sammendrag

Terroraksjoner med giftige kjemikalier er en trussel i dagens samfunn, og det er derfor svært viktig å ha god beredskap for håndtering og begrensning av skadene fra slike hendelser. En nøyaktig beskrivelse av utslipp og spredning av gifige kjemikalier, samt av mulige helseeffekter for individer som er utsatt for giften, er et viktig hjelpemiddel for en god beredskapsplanlegging.

Norge og Nederland inngikk i 2015 en samarbeidsavtale, “The Strategic Mutual Assistance in Research & Technology (SMART) on CBRN Protection”. Ett av flere prosjekter i dette samarbeidet er “CBRN Modelling & Simulation”, der målet er å kombinere modellerings og simulerings-kapabilitetene i Norge og Nederland til en felles kapabilitet til fordel for begge nasjoner. Denne rapporten beskriver arbeid som inngår i “SMART-CBRN Modelling & Simulation”-prosjektet.

Et scenario der nervegassen sarin blir spredt inne i en messehall er studert ved bruk av avanserte numeriske beregninger. To ulike modelleringsrutiner er brukt, med ulik grad av nøyaktighet og ulike behov til beregningsressurser og regnetid: large eddy simulations og Reynolds-averaged Navier-Stokes-simuleringer. Fordamping fra to små dammer på golvet blir beregnet med en analytisk modell, som avhenger av den simulerte luftstrømmen. Fordamping fra de to dammene blir simulert hver for seg, og mulige virkninger på mennesker tilstede i hallen blir anslått fra de resulterende konsentrasjonene av gass i messehallen.

Fordampingshastigheten avhenger sterkt av hvor væskedammen er plassert. Nær dammene kan milde helseeffekter som synshemmelser opptre innen få minutter, mens mer alvorlige helseeffekter ikke vil opptre før over en halv time etter at fordampingen har startet. Gassen blir ikke veldig effektivt transportert vekk i simuleringene. For simuleringene med fordamping fra dam 1, som ligger inne i et delvis lukket rom, tar det 10–30 minutter før farlige konsentrasjoner oppnås i naborommene. For simuleringene med fordamping fra dam 2, som ligger i gangen utenfor rommene, blir nokså lite gass transportert inn i rommene. I simuleringene er det sett bort fra publikums tilstedeværelse og bevegelse i hallen, men i en faktisk situasjon kan de påvirke spredningen av gass betydelig. Det er også noen porter direkte ut fra hallene, som er stengt i simuleringene. Dersom disse portene er åpne, vil spredningen av gass inne i hallene være mer effektiv enn simuleringene viser.

Large eddy simuleringer gir hastighetsfelt med større fluktuasjoner enn Reynolds-averaged Navier-Stokes-metoden, og gir trolig en mer realistisk simulering av gasstransporten i messehallen.

Resultatene fra simuleringene kan brukes som referansedata for simuleringer med andre modeller, for eksempel de to innendørs spredningsmodellene G-COMIS og CONTAM. De kan også benyttes for å utføre beredskapsøvelser og for planlegging av prosedyrer for håndtering av slike hendelser. Et nyttig steg videre i arbeidet med innendørs spredning, vil være å utføre eksperimenter, for å få referansedata som kan validere modellene.

Contents

Preface

Norway (FFI) and the Netherlands (TNO) have a collaborative effort named “The Strategic Mutual Assistance in Research & Technology (SMART) on CBRN Protection” ongoing since 2015. There are several projects within this collaboration. The work presented in this report is conducted within the project “CBRN Modelling & Simulation”, which started January ^{1st} 2016. The overall goal of the collaboration is to combine the CBRN modelling and simulation capabilities in the two institutes into an improved modelling and simulation capability for mutual benefit.

The CBRN Modelling and Simulation project is divided into three work packages:

- WP1: Systems approach to CBRN modelling and simulation. Lead: TNO.
- WP2: CBRN release, dispersion and effects modelling - Operational models. Lead: FFI.
- WP3: CBRN release, dispersion and effects modelling - Indoor dispersion. Lead: FFI.

This report presents work carried out for WP3.

1 Introduction

The threat of terrorist actions involving toxic chemicals is present in today's society. Toxic industrial chemicals as well as chemical warfare agents may be within reach for groups who would use them for causing injury. Chemical attacs have been carried out: one of the most infamous cases of chemical terror is the sarin attacks in Tokyo in 1995, where the cult Aum Shinrikyo dispersed sarin in the city's metro system causing injury and death [1]. There is therefore a need for appropriate emergency response planning in case of chemical terrorist attacks. This planning needs to be built upon a proper understanding of the threat itself, which is why scientific investigation into these types of accidents is important.

There are several methods available for modelling the release and dispersion of toxic gases and for assessing the possible consequences and outcomes. These differ in the time required for conducting the dispersion modelling and in the level of details that are resolved. A description of the general characteristics of various modelling efforts is give in [2]. In the work at hand, two Computational Fluid Dynamics (CFD) approaches are used. One of the methods used, Large Eddy Simulations (LES) is extremely computationally demanding, but can accurately describe details in the flow field and the dispersion of gases in complex geometries. The other method used, Reynolds-Averaged Navier-Stokes (RANS) simulation, is not as computationally demanding, but cannot to the same accuracy resolve details in the flow field. LES accounts naturally for the large scale unsteady mixing due to the large scale temporal and spatial variations even in statistically steady flows, while RANS can only account for these variations in statistically unsteady flows [3]. It is of interest to compare these modelling approaches, to see how well the dispersion patterns and the consequence assessment agree. It would also at a later time be interesting to compare these results with faster models which cannot resolve the same degree of details (for instance the indoor dispersion models G-COMIS or CONTAM).

This report describes a terror scenario with dispersion of sarin inside a convention centre which may host several hundred people. The dispersion patterns from two different release points are investigated along with the possible outcomes of the release in terms of physiological effects to people present in the convention centre at the time of release.

1.1 Sarin

Sarin is a nerve agent which, at ambient conditions, is an odour- and colourless liquid with a boiling point of 145°C [4]. Symptoms of intoxication will appear within minutes of exposure, and vary in severity from impaired vision (pin-point pupils, miosis), to runny nose and eyes to respiratory arrest and death [4]. Medical treatment exists, but should be administered quickly after exposure.

1.2 Scenario description

The convention centre in this work has been studied before with some differences in the geometry and the release mechanisms [3, 5]. The layout of the convention centre is shown in figure 1.1 and

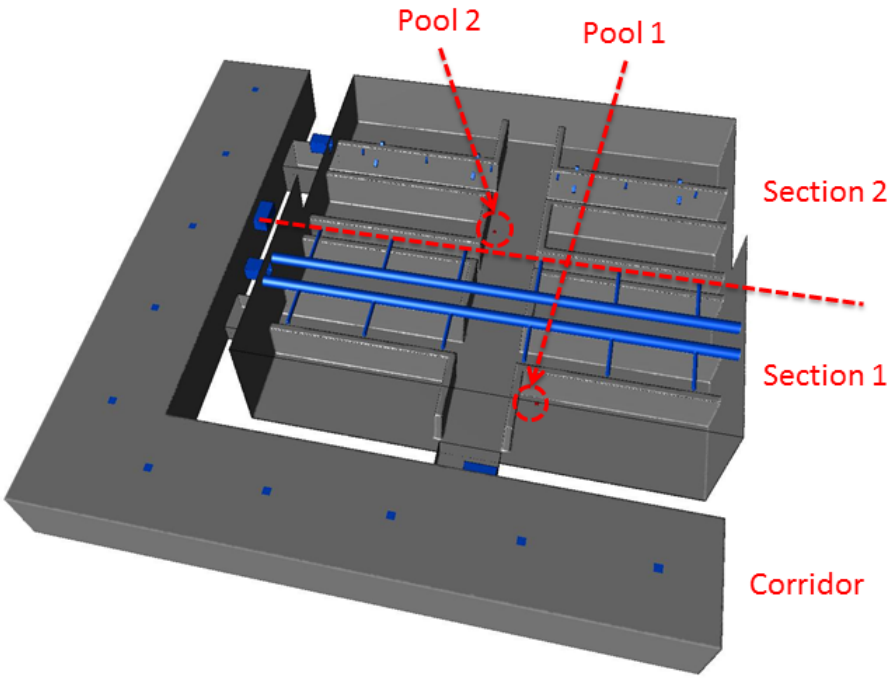

Figure 1.1 *View of the convention centre. The walls are gray and the ventilation system is blue. The rectangular parts of the ventilation system which are on the outside of the side walls belong to the ventilation outlet system, and the rest belong to the ventilation inlet system.*

1.2. The convention centre consists of three parts: section 1, section 2 and a corridor. Sections 1 and 2 each have an area of 1800 m^2, but section 1 has a ceiling height of 16.6 m and section 2 has a height of 9.8 m. Sections 1 and 2 are divided into in total eight semi-confined rooms, numbered 1 to 8, each seating approximately 100 persons. The walls between these semi-confined rooms extend 6 m above the floor with openings above. There is no other physical divide between sections 1 and 2. The corridor is connected to sections 1 and 2 by three passages, denoted as exit A, B and C. In addition to the passages to the corridor, there are gates in the back wall which can be opened for evacuation purposes, but these are taken to remain closed in the present scenario.

The ventilation system is divided into three parts, one for each section and one for the corridor, operating independently. The ventilation system is assumed to operate at full capacity. The total air flow through the ventilation system is 11.9 kg/s for section 1, 15.3 kg/s for section 2, and 15.3 kg/s for the corridor.

The source term for the scenario is 0.5 litre of liquid sarin poured on the floor to form a pool. It

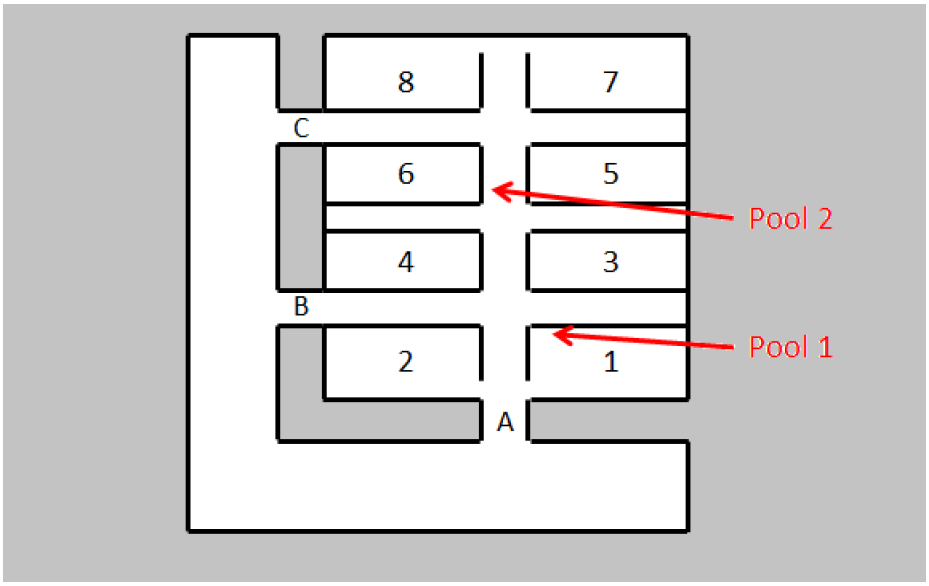

Figure 1.2 *Schematic view of the convention centre with labels on the different rooms. Section 1 is divided into rooms 1-4 and the hallway between the rooms and section 2 is divided into rooms 5-8 and the hallway between the rooms. Pool 1 is inside room 1 and pool 2 is in hall section 2. A, B and C are exits to the corridor.*

is assumed that the liquid surface from which sarin will evaporate has an area of 0.25 m^2 and a thickness of 2 mm. Two different locations for the spill are considered, one inside a semi-confined room, and one in the hall between the rooms (figure 1.2).

2 Mathematical modelling

2.1 General approach

In order to obtain a detailed and accurate description of the dispersion of sarin a good description of the air velocity field is needed. In this study, Computational Fluid Dynamics (CFD) has been applied to calculate the air velocity field in the convention centre, and thereafter applied to the dispersion of sarin. There are two different scenarios: evaporation from pool 1 and evaporation from pool 2, and two different CFD approaches are used: Large Eddy Simulation (LES) and Reynolds-Averaged Navier-Stokes (RANS). All calculations were performed using the FLUENT software [6].

2.2 CFD modelling

The motion of an incompressible fluid is described by the Navier-Stokes equations, 2.1 and 2.2, which describes conservation of momentum and mass respectively:

$$\rho\left(\frac{\partial u_i}{\partial t} + u_j\frac{\partial u_i}{\partial x_j}\right) = -\frac{\partial p}{\partial x_i} + \mu\left(\frac{\partial^2 u_i}{\partial x_j^2}\right) + f_i \tag{2.1}$$

$$\frac{\partial u_i}{\partial x_i} = 0 \tag{2.2}$$

where ρ is the fluid density, u the velocity, t time, x the spatial coordinates, p the pressure, μ the dynamical viscosity of the fluid, and f external forces (for instance gravity). The subscripts (i and j) denote the three spatial directions. The Navier-Stokes equations have no general analytical solution, and have to be solved numerically on computational meshes, where the computational domain is divided into a number of computational cells; the equations describing the fluid motion are solved for each cell. In some cases equations 2.1 and 2.2 can be solved exactly by Direct Numerical Simulations (DNS), but in practice this is only feasible for small geometrical domains and fairly low velocities. In practice a turbulence model has to be included to solve the set of equations. A detailed description of the turbulence models is given in for instance [7], a brief description is given in appendix A.

2.2.1 Computational details

2.2.1.1 Computational grids

Two different computational grids are used. Computational grid 1 consists of approximately 23 million cells, with a spatial resolution ranging from approximately 4 cm to 30 cm. This is used for both LES and RANS simulations. Computational grid 2 is smaller, with approximately 8 million cells and a resolution that ranges from approximately 8 cm to 60 cm. This is used for RANS only. The highest resolution is located beneath the ventilation inlets and above the evaporation pools in both grids.

2.2.1.2 CFD details

The boundary conditions on the ventilation inlets and outlets were specified according to the description of the convention centre in section 1.2. No-slip boundary conditions were applied on the solid surfaces. The vapour sources were specified as velocity inlets, where the velocity of the vapour was calculated with the evaporation model described in section 2.2.2.

Three sets of simulations were performed with different computing approaches:

- In the first computational approach, LES was applied on computational grid 1. Evaporation from pool 1 and pool 2 separately were simulated. The time step for the simulations were 0.12 seconds and a second order implicit time stepping procedure was used. The air velocity field was allowed to develop for 90 minutes real time, after which it appeared stable. A that time the evaporation model was applied to either pool, and the evaporation was allowed to continue for another 60 minutes real time before the simulations were terminated.
- In the second computational approach, RANS simulations were performed on computational grid 1, this approach was only used for evaporation from pool 1. The time step used was 0.3 seconds and a second order implicit time stepping procedure was used. The air velocity field was allowed to develop for 60 minutes, after which it appeared fully developed. The evaporation model was applied for further 60 minutes until the simulations were stopped.
- In the third computational approach, RANS simulations were performed on computational grid 2. This approach was applied for evaporation from both pools, separately. The time step was 1.0 second and the velocity field was allowed to develop for 60 minutes, after which it appeared fully developed. The evaporation model was applied to each of the pools for 60 minutes after which the simulations were stopped.

The calculated evaporation rates were so low that the accordingly low vapour concentrations led to severe numerical diffusion problems in the simulations. It was therefore decided to multiply the evaporation rate calculated by the model by 1000 (in one case 10 000) in order to circumvent these problems.

The density of sarin is greater than that of air, but due to the very low concentrations of sarin that are relevant in this study, the sarin-air mixture will effectively behave as a neutral gas (density similar to that of air). However, upscaling the concentration by a factor of 1000 (or 10 000) could severely affect the density and therefore also the transport of the gas. In order to avoid this problem, the sarin release was simulated as release of a neutral gas with all the same properties as air.

By increasing the evaporation rate, the velocity of the vapour entering the domain will also increase. However, after the upscaling, the mass flow of vapour due to evaporation is still three orders of magnitude lower than the mass flow of the ventilation system, and the vertical velocities above the pool is less than 0.01 m/s. Because the velocity is so low, and because the sarin release is simulated as a neutral gas release, the vapour will not affect the ambient velocity field from the ventilation system, and the results correspond to the specified scenarios.

The evaporating liquid pool was implemented in the simulations as a velocity boundary condition, hence the volume fraction of the simulant gas corresponds to the volume fractions of sarin. The volume fractions were converted to sarin concentrations by use of the actual mass density of sarin

during post processing of the data. The application of air as sarin simulant means that the diffusion coefficient of the gas is incorrect, but this effect is expected to be negligible compared to the effect from turbulence and the air velocity field for the dispersion of vapour.

The presence and movement of people in the convention halls are disregarded in the simulations. Since the velocities at ground level are very small, the air velocity caused by people moving might not be negligible. For the calculation of received doses, mean values in the various rooms are used and should diminish the error of neglecting the presence and movement of people somewhat. The movement of people, however, might also lead to an increased evaporation rate, and thus larger concentrations of vapour in the rooms.

Additionally, deposition of sarin on surfaces is neglected in these calculations, which will lead to over-prediction of vapour in the air. The effect of temperature gradients in the room on the dispersion process is also neglected.

2.2.2 Modeling evaporation

The evaporation model used in this study is developed by Vik and Reif [8] and referred to in their work as model B, applicable for larger liquid surfaces. This model is really developed for droplets or small pools, not for pools as big as in the current simulation. Furthermore the model includes two model variables which are parametrized for experimental measurements of a different substance, it could be that these could to some extent be specific to the chemical. However, the model should have a functional dependence on the friction velocity, and the results should be scalable.

In this model, the evaporation rate from a pool is dependent on the shear friction velocity, u_*, which is related to the shear stress on the liquid surface, τ, by:

$$\tau = \rho u_*^2 \tag{2.3}$$

The friction velocity can also be computed from the velocity gradient near the surface:

$$u_* = \sqrt{\nu \left(\frac{\partial U}{\partial z} \right)_{z=0}} \tag{2.4}$$

The amount of evaporated mass, m_e, as function of time, t, is given by:

$$m_e = v_v A_0 \int_0^t C dt' \tag{2.5}$$

where v_v is a vapour velocity (which is equal to the friction velocity, u_*, for model B), A_0 is horizontally projected area of the liquid surface. The concentration above the surface, C, is calculated by:

$$C\left(u_*, t\right) = C_0 \mathcal{G} \frac{u_*}{\nu} \exp\left(-\mathcal{H} t^2\right) \tag{2.6}$$

where C_0 is the saturation concentration. $\mathcal{H}$ and $\mathcal{G}$ are model coefficients given by:

$$\mathcal{H} = \frac{C_0 \lambda A_0 u_*^3}{4 m_0 \nu} \tag{2.7}$$

and

$$\mathcal{G} = \frac{1}{K}\frac{2m_0\nu\sqrt{\mathcal{H}}}{C_0 u_*^2 A_0\sqrt{\pi}} \tag{2.8}$$

where m_0 is the original liquid mass. λ and K are model parameters which were fitted to experimental data in the work of Vik and Reif [8]. The model has been applied "as is" in the present work and has been implemented in FLUENT by a user defined function.

In the simulations, the vapour source of the liquid surface is defined as a velocity inlet boundary condition. The evaporation rate, $q_e = \Delta m/\Delta t$, is calculated from equations 2.5 and 2.6, and the resulting velocity boundary condition as:

$$u_{bc} = \frac{q_e}{A_0\rho} \tag{2.9}$$

2.2.3 Consequence assessment

In order to assess the consequences to the public from sarin vapour inhalation, the probability of miosis, incapacitation and death are calculated from the so-called toxic load model, developed by TNO. For a description of the use of the model, see [9]. This model calculates the probability of various effects based on the time varying airborne concentration. It takes into account the fact that different individuals have different responses to toxic hazards, that there can be large variations in the concentrations, and that the available toxicological data are not always able to predict a dose-response. The toxic load, TL, is given by:

$$TL = \int_0^{t_e} C^n dt \tag{2.10}$$

for a time varying concentration, $C(t)$, for a time of exposure t_e. The exponent n is material specific. The probability for a given effect is given by:

$$P = \frac{1}{2} + \frac{1}{2}erf\left[\frac{b}{\sqrt{2}}\ln\frac{TL}{TL_{50}}\right] \tag{2.11}$$

where b is related to the standard deviation of the log-normal distribution and TL_{50} is the toxic load that causes 50% of the population to experience the given effect. The toxic load variables in table 2.1, taken from [10], are used for the consequence assessment.

Miosis			Incapacitation			Death		
ICt_{50} (10 minutes) ($mg \cdot min/m^3$)	b	n	ICt_{50} (10 minutes) ($mg \cdot min/m^3$)	b	n	LCt_{50} (10 minutes) ($mg \cdot min/m^3$)	b	n
2.5	2.1	2	15	4.3	1.3	35	5.2	1.3

Table 2.1 *Concentrations over time of sarin which give ocular or incapacitating effects (ICt_{50}) and life threatening effects (LCt_{50}) in 50 % of the population after 10 minutes exposure, and the values of the exponent n in equation 2.10 and the parameter b in equation 2.11. The data are taken from [10].*

Spatial averages of the concentrations at a height 1 m above the floor are calculated in each room, in each hall section, and in the corridor in the convention centre. Doses and toxic loads are calculated from these spatial mean concentrations. The probabilities for the specified health effects are then calculated with equation 2.11. Probabilities from doses is calculated from the time integrated concentrations instead of TL, and with ICt_{50} and LCt_{50} instead of TL_{50}.

3 Results

3.1 Velocity field

Figure 3.1 shows the mean velocity field in a plane one meter above the floor in the entire convention centre for the LES simulations. The velocities close to the floor are relatively small. There is a velocity flux into the hall from the corridor through exit A, while through exit B and C the velocity field is more complex. The mean velocity field for the RANS simulations are shown in figure 3.2. Mostly the same structures are seen in all velocity fields, but LES produce additional smaller structures to those from the RANS simulations.

Figure 3.3 shows the vertical component of the velocity in a plane through the ventilation inlets which have the largest inflow velocities. The vents produce jets of air that extend almost all the way to the floor, for LES the vertical velocity is still approximately five m/s six meters above the floor, though the high velocity jets are very narrow. The RANS simulations produce more diffuse jets, for which the highest velocities do not extend as far down as in the LES. This is the case for all the inlet vents in the convention centre.

In reality ventilation inlets are not openings straight into the rooms; there is usually an obstruction impinging the inflow or the air flow is channeled through the openings with a certain angle. In order to assess the importance of this approximation, a RANS simulation was conducted in which the inlet boundary conditions in section 1 were changed from simple vertical inlet vents to a conical shape at an angle of 60 degrees from the vertical line. The main aspects of the velocity field remained the same, although the resulting velocity field was more diffuse in that the jets grew wider and the velocities in the jets subsided quicker. Near the ground, the velocity field was unchanged from the simulations with straight jet.

3.2 Evaporation

The average evaporation rates for each simulation and the total amount evaporated during one hour are given in table 3.1. LES produced larger evaporation rates than the RANS simulations, leading to overall larger sarin concentrations in the LES results. This could be partially due to how the shear velocity gradient is modelled in the two approaches. For LES, the velocity gradient is given by solving the equations in section A.1, while the RANS simulations involve wall functions to model the velocity gradient near the wall. The results in the former case is highly dependent on the grid resolution. On the other hand, the differences in the velocity fields seen in figure 3.3, where LES has straight jets reaching almost to the floor, can also affect the evaporation rate. The RANS simulations on the two grids gave similar results for the evaporation rate.

Pool 1 had a larger evaporation rate than pool 2. This is due to the different locations and the differences in the velocity field. The local velocity field around pool 1 yields larger shear stress than the local field around pool 2. Figures 3.1 and 3.2 indicate that the velocities around pool 1 are higher than around pool 2.

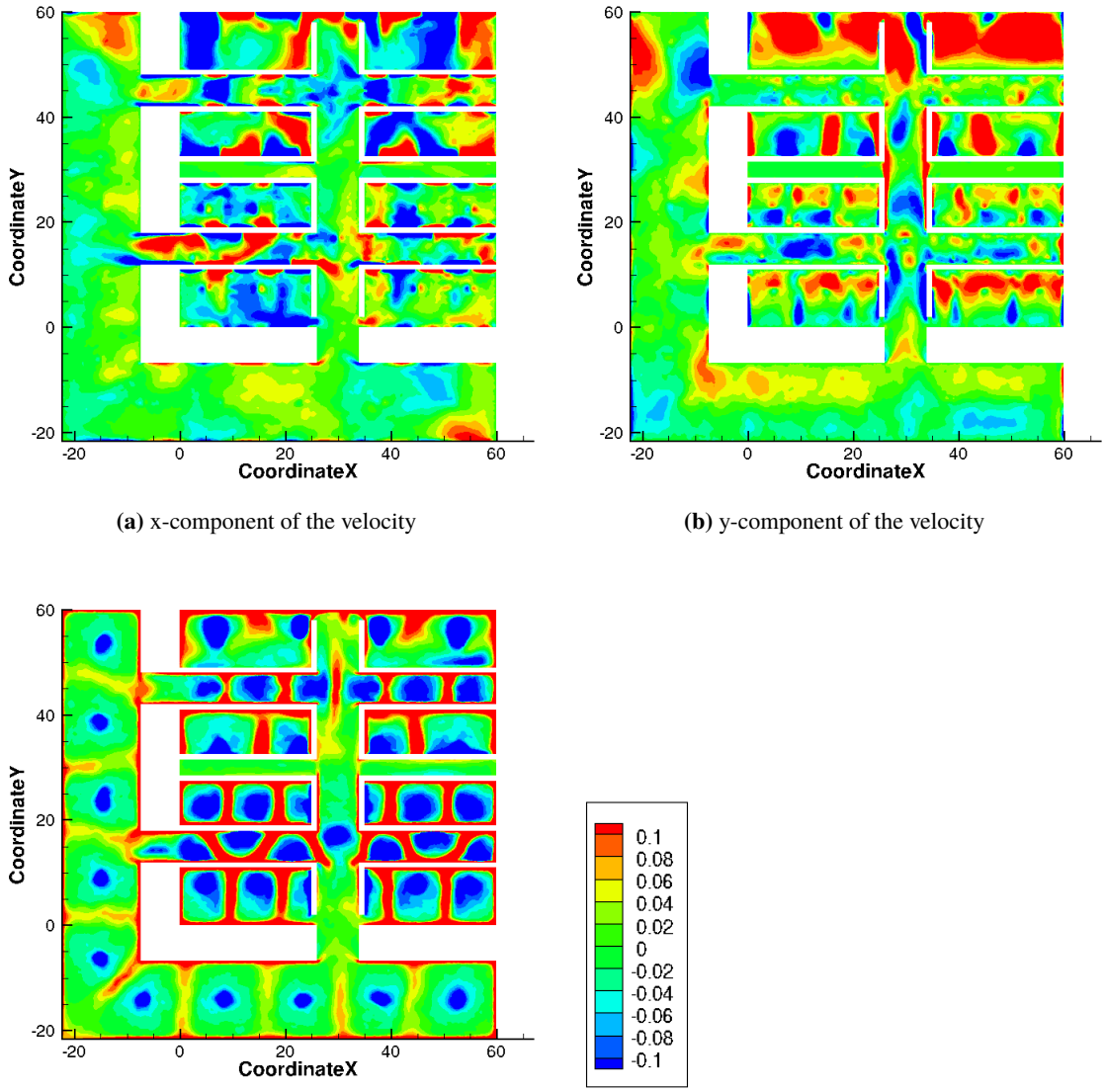

(a) x-component of the velocity

(b) y-component of the velocity

(c) z-component of the velocity

(d) Colour legend

Figure 3.1 *Mean air velocity field for LES displayed in a horizontal plane 1 m above the floor.*

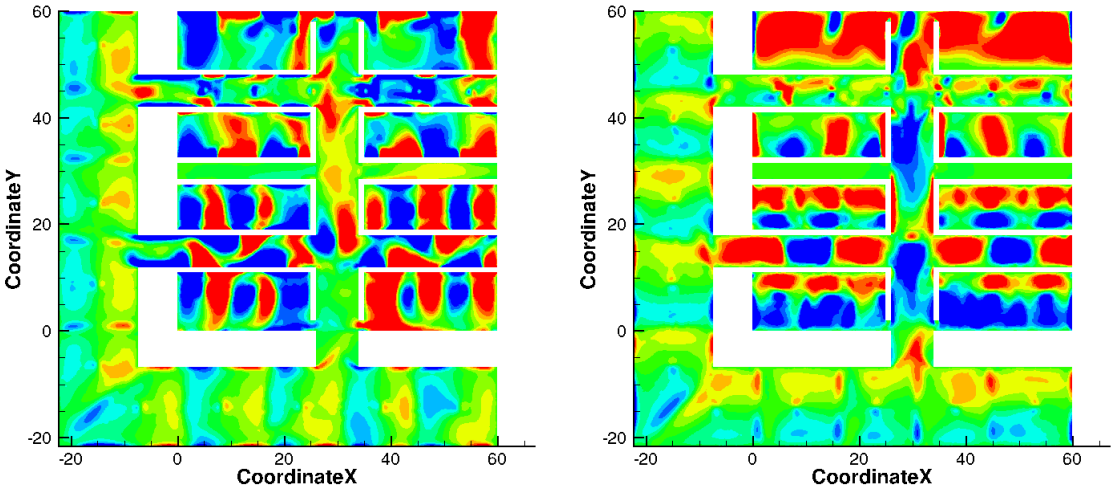

(a) x-component of the velocity, grid 1

(b) y-component of the velocity, grid 1

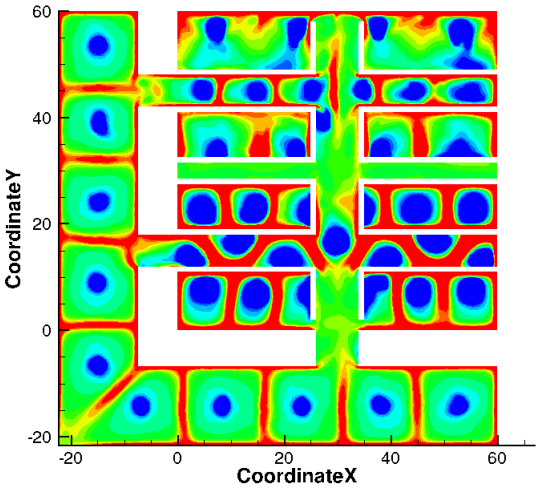

(c) z-component of the velocity, grid 1

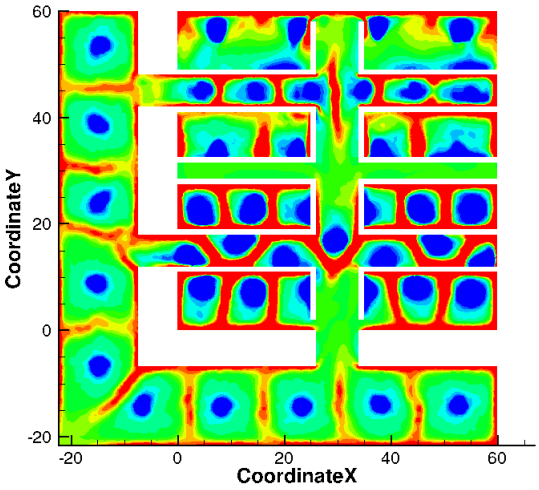

(d) z-component of the velocity, grid 2

Figure 3.2 *Mean air velocity field for RANS displayed in a horizontal plane 1 m above the floor. Figure (a), (b) and (c) shows the three velocity components for grid 1, while (d) shows the z-component (vertical component) for the simulation with grid 2. The colour scale is identical as for figure 3.1 (-0.1, 0.1).*

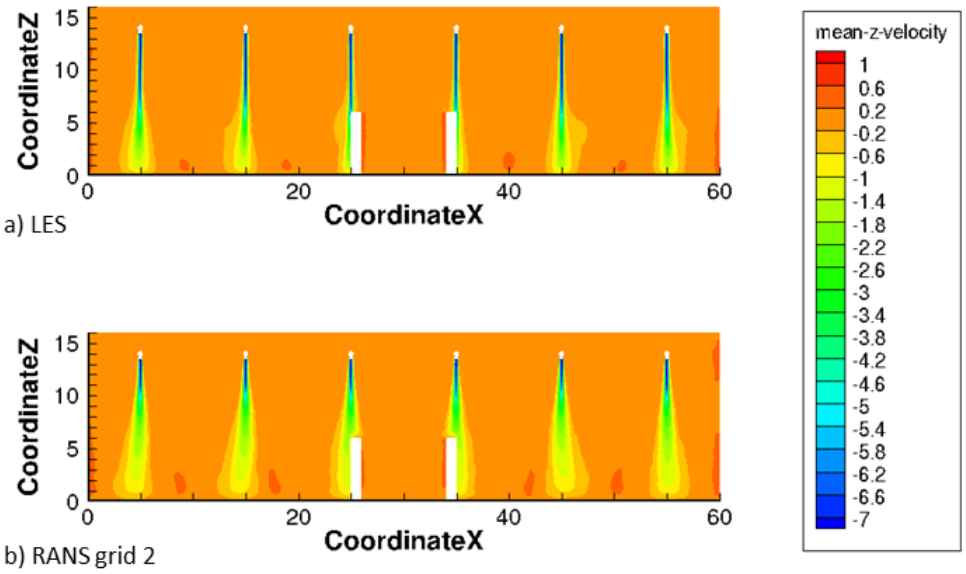

Figure 3.3 *Mean vertical velocity (m/s) in a vertical plane perpendicular to the y-direction, through ventilation inlets in hall section 1. Top: LES, bottom: RANS simulations on grid 2. The white elements are separation walls between rooms 3 and 4.*

Simulation	Average evaporation rate (mg/s)		Total amount evaporated (g)	
	Pool 1	Pool 2	Pool 1	Pool 2
LES on grid 1	5.39 (1.87)	1.67 (0.64)	19.42	6.02
RANS on grid 1	3.20 (0.87)	-	11.53	-
RANS on grid 2	3.13 (0.22)	0.38 (0.091)	11.25	1.37

Table 3.1 *Average evaporation rates over the first hour after spill (mg/s), standard deviations in parenthesis), and the total amount evaporated during one hour (g).*

The evaporation rates were overall steady during the entire time of all simulations, although there were considerable fluctuations around the mean, especially for LES. A steady evaporation rate is considered reasonable as only small fractions of the liquid pools evaporate during the simulation.

3.3 Dispersion

Figure 3.4 displays the concentrations of sarin in a plane one meter above the floor in the entire convention centre after 10, 30 and 60 minutes for the LES and RANS simulations with evaporation from pool 1. The highest concentration of sarin is found in room 1 where the pool is located (LES predicts an average concentration of about 1 mg/m^3 in this room). The vapour then disperses into the hall of section 1 and into room 2 before it spreads out into the corridor through exit B and into rooms 3-4 and section 2. The part of the corridor outside exit A remains the area with the lowest concentrations of sarin throughout the simulations, even though the concentration just inside the exit

gets fairly high. The reason for this is apparent from the velocity fields above: the wind flows into the hall form the corridor through exit A. The main transportation of sarin into the corridor occurs through exit B in every simulation. Over all there is fairly good agreement between all simulations.

Figure 3.5 displays the concentrations of sarin in a plane one meter above the floor in the entire convention centre after 10, 30 and 60 minutes for the LES and the RANS simulation with evaporation from pool 2. In this case, the largest concentrations are located in the middle of the convention centre hall near the pool. The rooms nearest the pool (room 3, 4, 5 and 6) get concentration levels of about 2–3 times higher than the other four rooms, but none of the rooms reach the high concentration levels observed near the pool.

Figure 3.6 and 3.7 shows the spatial average concentrations in a plane one meter above the floor in the nearest four rooms for each of the cases. The RANS simulations appear to reach a quasi-steady state after approximately 40 min, where the concentrations inside the rooms cease to increase even though the concentrations here are lower than in the hall outside the rooms (not shown); after some time, as the evaporation start to decrease and in the end terminates, the concentration levels will decrease also. Because of the higher evaporation rate, LES shows overall higher concentrations than the RANS simulations. After one hour, the average concentration in the hall appears to be stable, but the concentration in rooms 1-8 and the corridor outside exits B and C are still increasing. It therefore does not appear to be a quasi-steady state yet. Even so, the simulation was terminated at this point in time due to the huge computational resources and time required for these simulations. Furthermore, it is assumed that in a real incident, the convention centre would be evacuated at this point.

There are huge fluctuations around the average concentrations. Figure 3.8 shows the average concentration with error bars in room 1 from the LES with evaporation from pool 1 and in room 3 for the RANS simulation (the error bars are truncated below $C = 0$). The error bars show the standard deviation of the spatial concentration field:

$$\sigma = \sqrt{\frac{\sum_{i=1}^{n} (c_i - \overline{c})^2}{n}} \tag{3.1}$$

where c_i is the concentration at position i, n the number of "read out" positions, and $\overline{c}$ is the spatial average concentration. The standard deviation is of the same size for LES and RANS; they are shown on separate figures for visual clarity.

In room 3 there is a huge difference in the average concentration in the two RANS simulations, larger than the standard deviation. This difference is also evident in figure 3.4 at 30 and 60 minutes. This can indicate that mesh independence in not reached, that is the mesh resolution affects the results.

3.4 Exfiltration

The exfiltration rates, that is the mass flow rate of sarin through the ventilation outlets, will be important to anyone standing outside the building. Figure 3.9 displays the exfiltration rates through the outlets in the convention halls and the corridor. Table 3.2 lists the instantaneous exfiltration

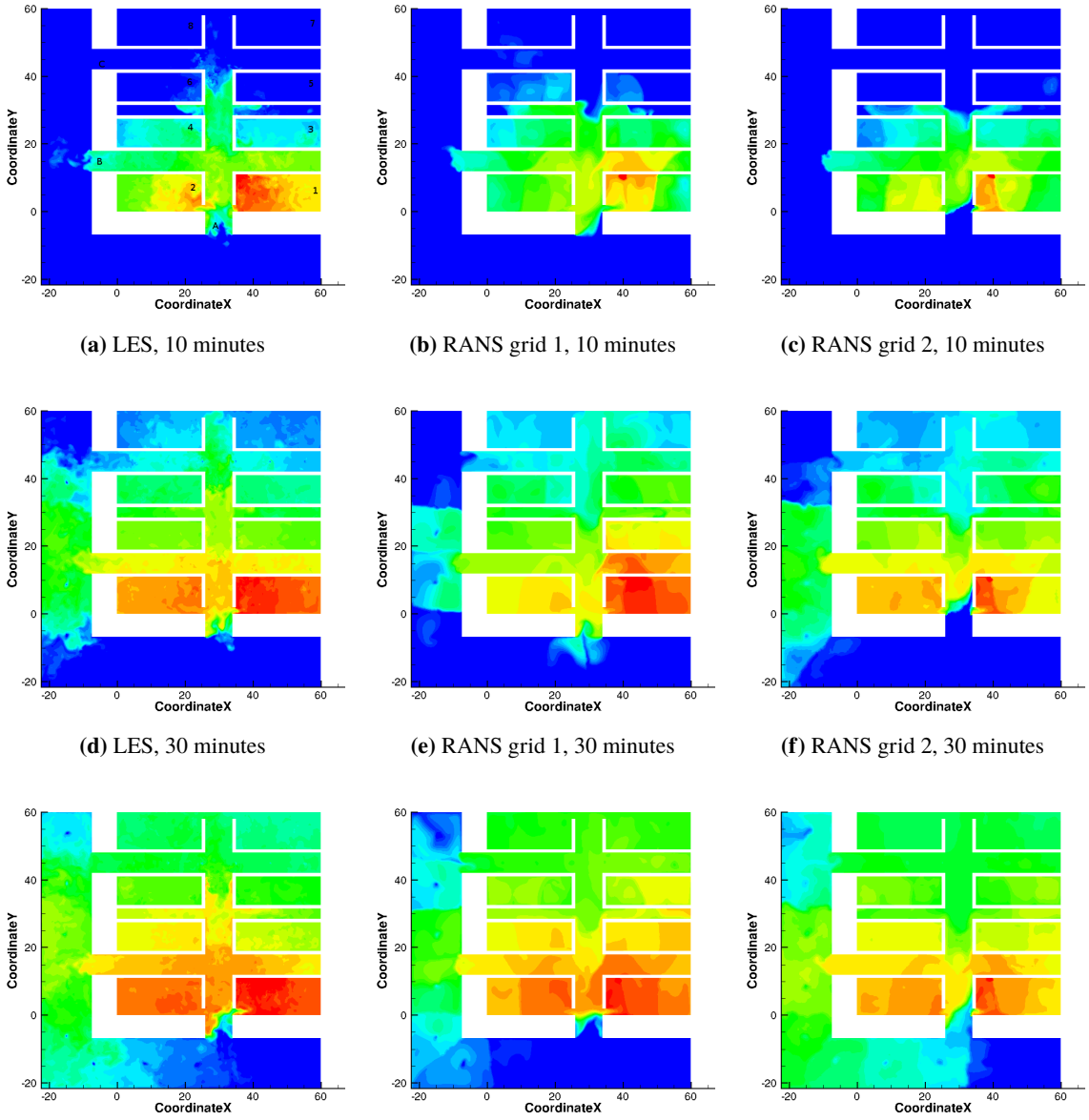

(a) LES, 10 minutes **(b)** RANS grid 1, 10 minutes **(c)** RANS grid 2, 10 minutes

(d) LES, 30 minutes **(e)** RANS grid 1, 30 minutes **(f)** RANS grid 2, 30 minutes

(g) LES, 60 minutes **(h)** RANS grid 1, 60 minutes **(i)** RANS grid 2, 60 minutes

Figure 3.4 *Concentrations of sarin (mg/m^3) in a plane 1 meter above the floor 10, 30 and 60 minutes after spill at pool 1. The colour levels show the concentration from light blue ($< 0.001\ mg/m^3$), through green, yellow and orange to red ($> 1\ mg^3$).*

Simulation	Exfiltration rate (mg/s)	
	Pool 1	Pool 2
LES on grid 1	4.20	1.57
RANS on grid 1	3.31	-
RANS on grid 2	2.96	0.55

Table 3.2 *Exfiltration rates one hour after start of the release.*

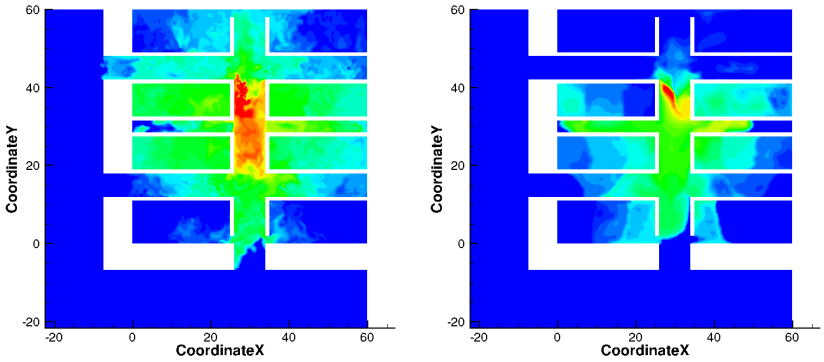

(a) LES, 10 minutes

(b) RANS grid 2, 10 minutes

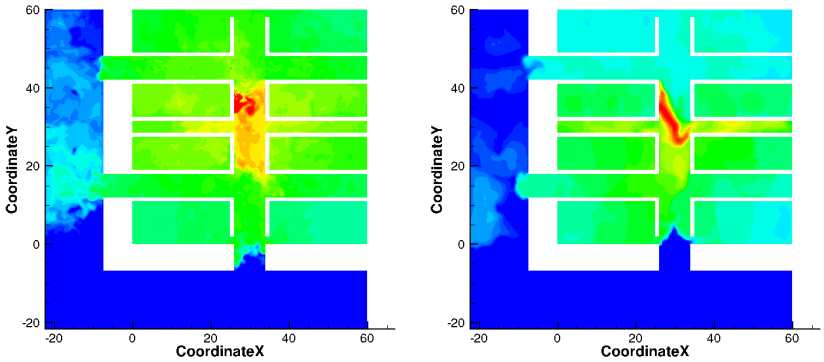

(c) LES, 30 minutes

(d) RANS grid 2, 30 minutes

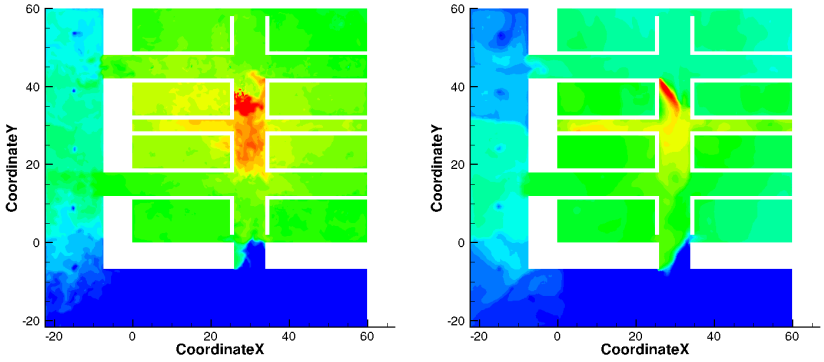

(e) LES, 60 minutes

(f) RANS grid 2, 60 minutes

Figure 3.5 *Concentrations of sarin (mg/m^3) in a plane 1 m above the floor 30 and 60 minutes after spill at pool 2. The colour levels show the concentration from light blue (< 0.001 mg/m^3), through green, yellow and orange to red (> 1 mg^3).*

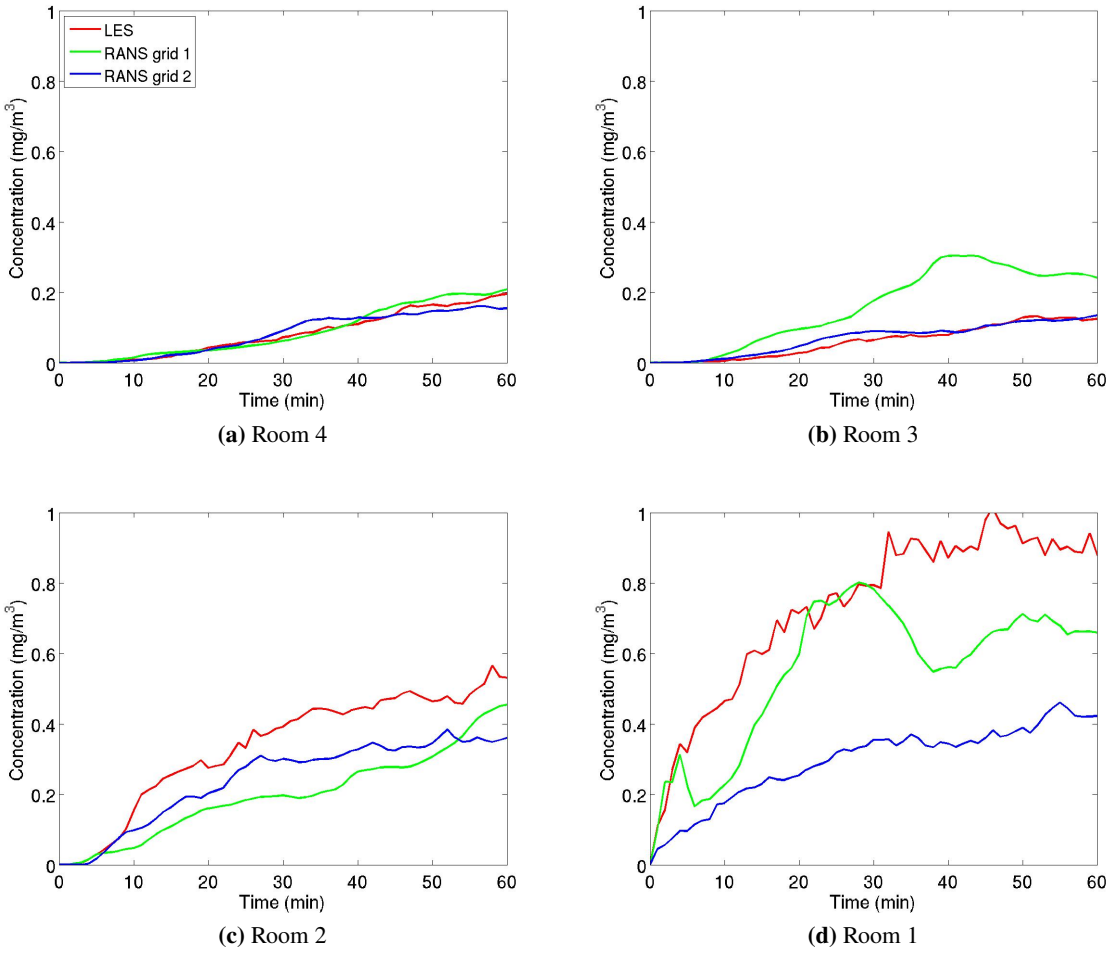

(a) Room 4 **(b)** Room 3

(c) Room 2 **(d)** Room 1

Figure 3.6 *Spatial average concentrations one meter above the floor for room 1, 2, 3 and 4 with evaporation from pool 1.*

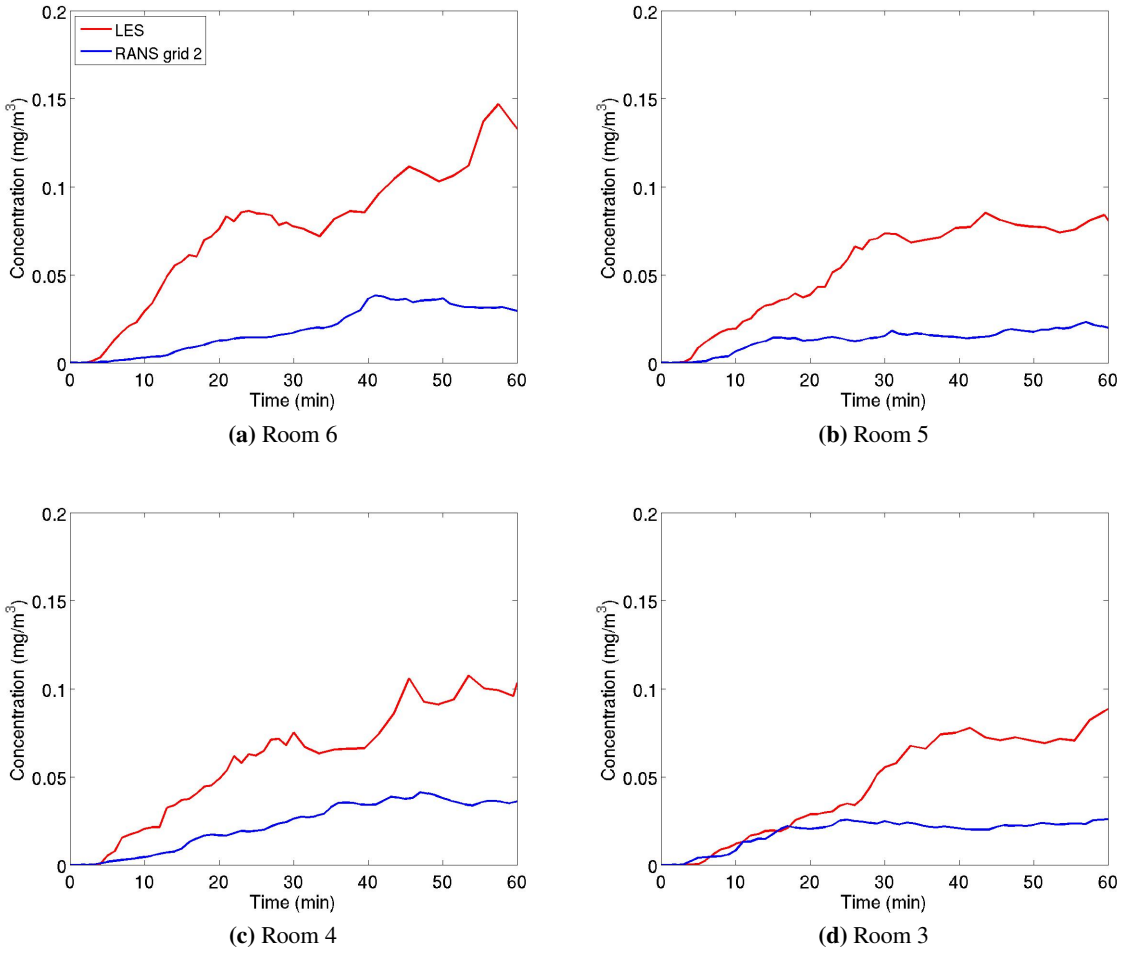

(a) Room 6 **(b)** Room 5

(c) Room 4 **(d)** Room 3

Figure 3.7 *Spatial average concentrations one meter above the floor for room 3, 4, 5 and 6 with evaporation from pool 2.*

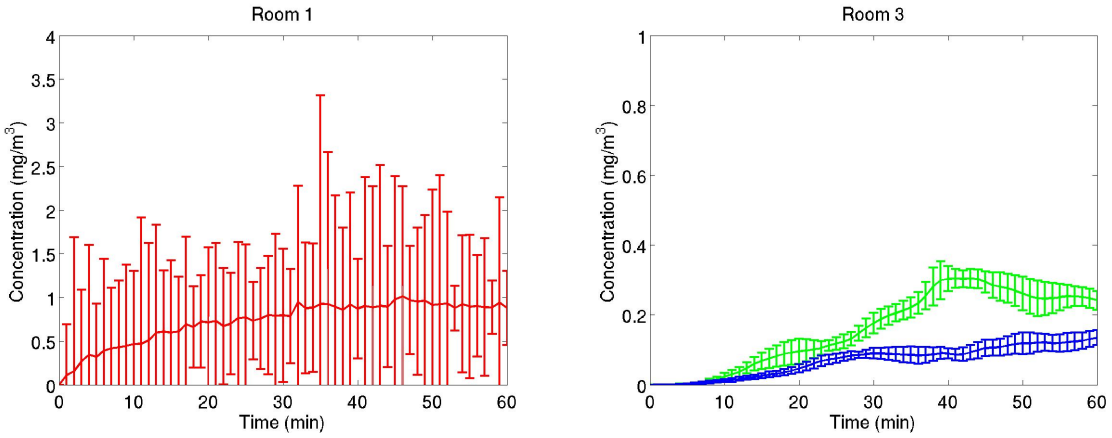

(a) LES **(b)** RANS

Figure 3.8 *Spatial average concentration and error bars (standard deviation) in room 1 for the LES and room 3 for the RANS simulations (the green line is grid 1, the blue line is grid 2) with evaporation from pool 1.*

rates one hour after start of the release These results can be used an input for a simulation of the dispersion in the area around the center.

For the case of evaporation from pool 1, LES predicts that about 80 % of the sarin disappears through the section 1 ventilation outlet, 10 % exits through the section 2 outlet and the remaining 10 % exits through the two outlets in the corridor. For the RANS simulations the corresponding exfiltration rates is about 75 % from section 1, 15 % from section 2, and the remaining 10 % exits through the corridor outlets.

In the case of evaporation from pool 2 both the LES and RANS simulations have less than 10 % exfiltration through the ventilation in the corridor after one hour. In the RANS simulation, the rest is divided almost equally between the outlets in sections 1 and 2, whereas in the LES,l the exfiltration is divided by approximately 65 % through the section 2 outlet and 35 % through the section 1 outlet.

For the RANS simulations, it appears that the outflow of sarin is equal to the inflow after 50-60 minutes. This indicates that a steady state has been reached in which the exfiltration rates should not increase significantly even if the evaporation is allowed to continue. In the LES, the exfiltration rates are still increasing after one hour.

3.5 Onset of symptoms

As described in section 1.2, the convention halls are divided into rooms 1-8 and hall sections 1 and 2 (see figure 1.2). Additionally the corridor was analysed as two parts: the part outside exit A and the part outside exit B and C. For each of these 12 parts of the convention centre, spatial average concentrations in a plane one meter above the floor are calculated (some of which are shown in figures 3.6 and 3.7), and from these doses, toxic loads and probability of observed physiological effects are calculated.

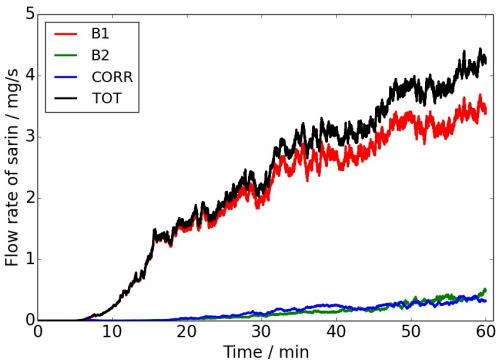

(a) LES, evaporation from pool 1

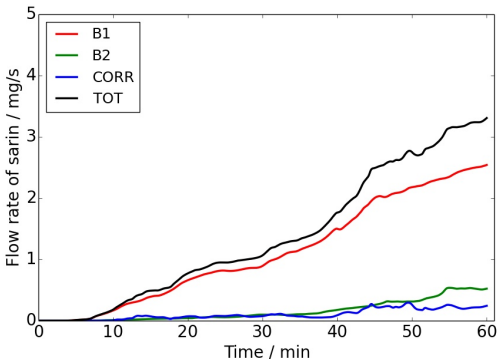

(b) RANS grid 1, evaporation from pool 1

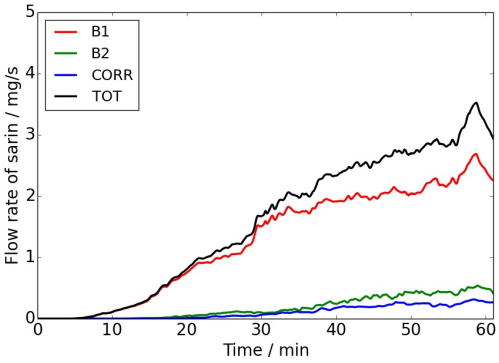

(c) RANS grid 2, evaporation from pool 1

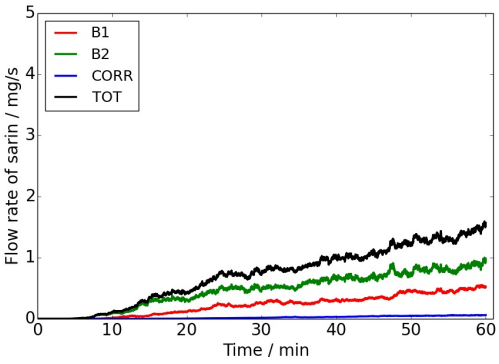

(d) LES, evaporation from pool 2

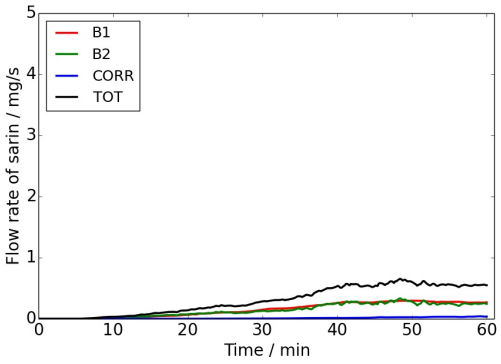

(e) RANS grid 2, evaporation from pool 2

Figure 3.9 *Exfiltration rates of sarin through the ventilation system (mg/s) as a function of time. The black line shows the total exfiltration from the convention centre, and the red, green and blue lines show the components of the exfiltration through the ventilation outlets in section 1, 2 and the corridor respectively.*

Three effects of the exposure to sarin are considered: miosis, incapacitation and death. The probabilities for the various effects as functions of time for the most relevant rooms are shown in figures 3.10, 3.11, 3.12 and 3.13. For the case of evaporation from pool 1 the probabilities calculated from the different simulations are in fair agreement, but with some internal differences. The RANS simulations predict slower onset of effects in the regions closer to the pool, but earlier onset in areas farther from the pool. It can also be seen that even though miosis effects are expected in large regions of the convention centre, there is apparently a time delay of about 30 min before the more severe effects will occur. Deadly doses are not expected to occur during the time of the simulations, except possibly in room 1 for evaporation from pool 1.

For room 3 the onset of miosis is predicted to occur much earlier in the RANS simulation with grid 1 than with grid 2. For incapacitation and death, the RANS simulations on grid 2 consistently predicts much later onset than RANS simulations in grid 1. This is related to the differences seen in the mean concentration in figure 3.6, and indicates that the grid resolution is an important factor, and that the resolution for grid 2 is too coarse.

In the scenario with evaporation from pool 2 the onset of miosis is predicted to occur after approximately 15 min in the area closest to the pool. The concentrations in this case are so low that incapacitation or death is not probable within the first hour. In the case of evaporation from pool 2 there is a fairly large difference between the predictions based on LES and RANS simulations. This is due to the much lower evaporation rate in the latter simulations.

For evaporation from pool 1, the onset of miosis is predicted to occur earlier when calculated with toxic load than doses, while for the other effects the onset is predicted earlier with dose than toxic load. This is is accordance with the calculations in reference [9] where it was shown that probabilities of effects based on toxic load is earlier if the concentration is greater than the reference concentration and later for the opposite situation. In the current simulation with evaporation from pool 1, the concentrations in the nearest rooms are generally greater than the reference concentration for miosis, but less than the reference concentration for incapacitation and death. For pool 2, the concentration is about the same as the reference concentration for miosis for LES, while RANS yield concentrations that are lower than the reference concentration.

The consequence assessment is based on average concentration values. As shown in figure 3.8, however, there are huge fluctuations in the concentration field, giving much higher concentration in some areas at times, as well as other areas with lower concentration.

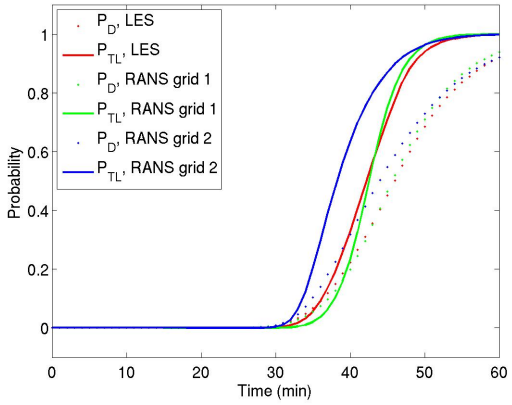

(a) Room 4

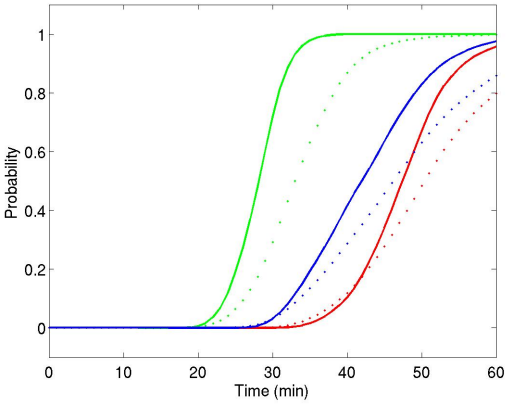

(b) Room 3

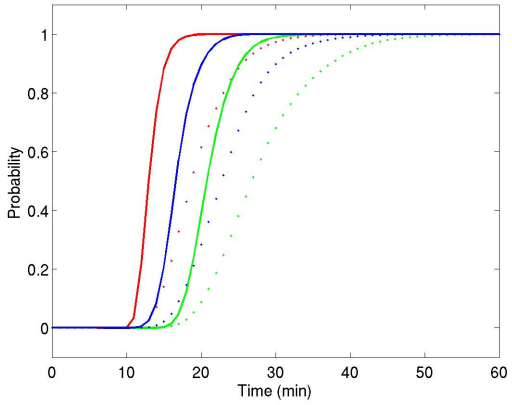

(c) Room 2

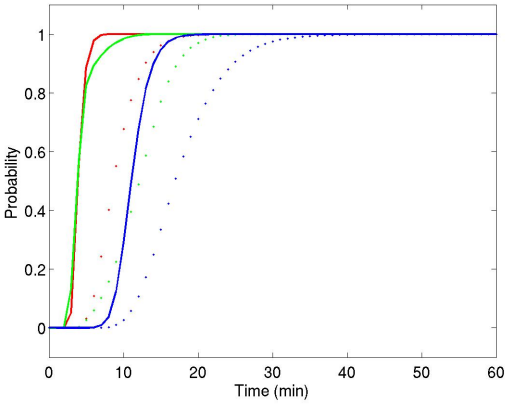

(d) Room 1

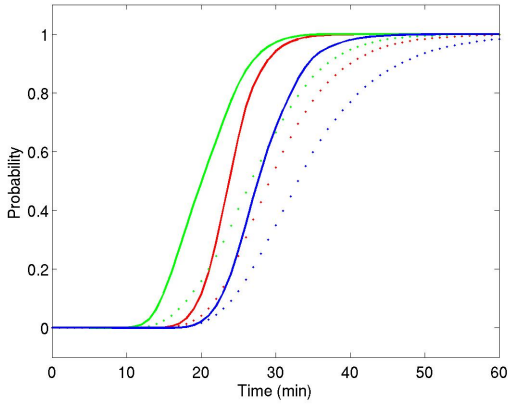

(e) Hall B1

Figure 3.10 *Probability of miosis in the public as a function of time after spill at pool 1. Red symbolizes LES, green and blue symbolizes RANS simulations on grid 1 and 2 respectively. The dotted lines indicate probabilities calculated from dose (P_D) and the full lines probabilities from toxic load (P_{TL}).*

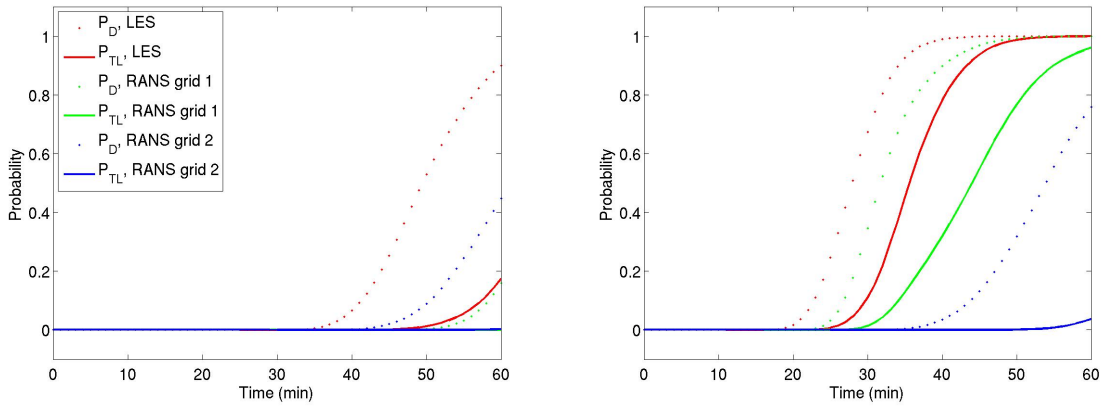

(a) Room 2 **(b)** Room 1

Figure 3.11 *Probability of incapacitation in the public as a function of time after spill at pool 1. Red symbolizes LES, green and blue symbolizes RANS simulations on grid 1 and 2 respectively. The dotted lines indicate probabilities calculated from dose (P_D) and the full lines probabilities from toxic load (P_{TL}).*

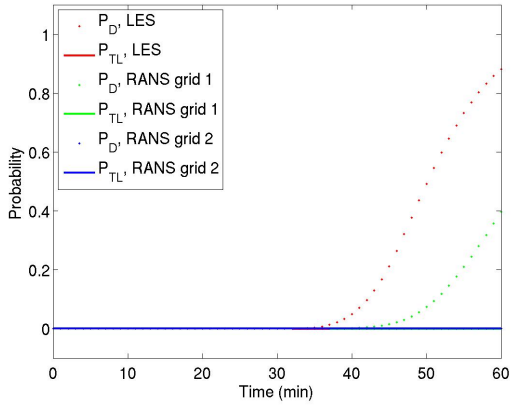

(a) Room 1

Figure 3.12 *Probability of death in the public as a function of time after spill at pool 1. Red symbolizes LES, green and blue symbolizes RANS simulations on grid 1 and 2 respectively. The dotted lines indicate probabilities calculated from dose (P_D)and the full lines probabilities from toxic load (P_{TL}).*

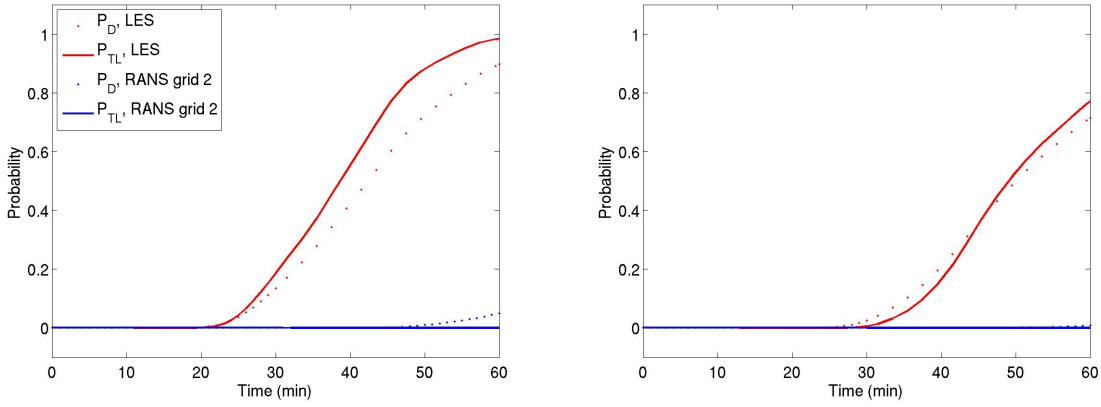

(a) Room 6

(b) Room 5

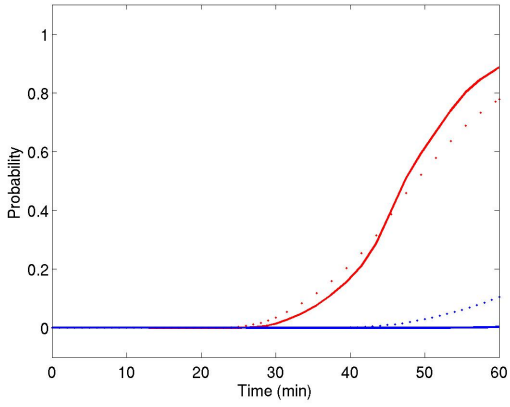

(c) Room 4

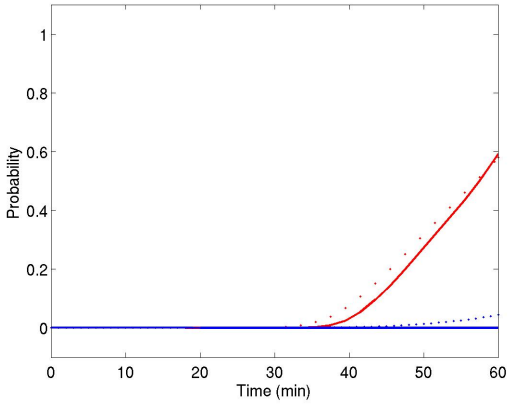

(d) Room 3

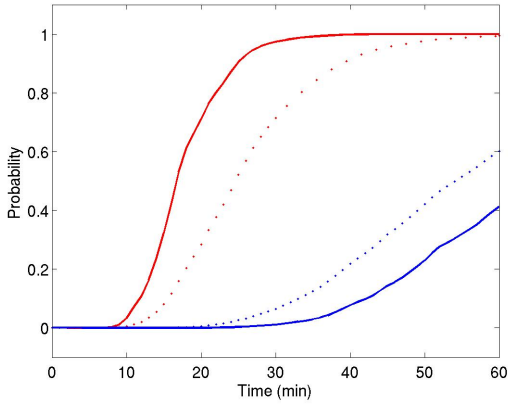

(e) Hall B2

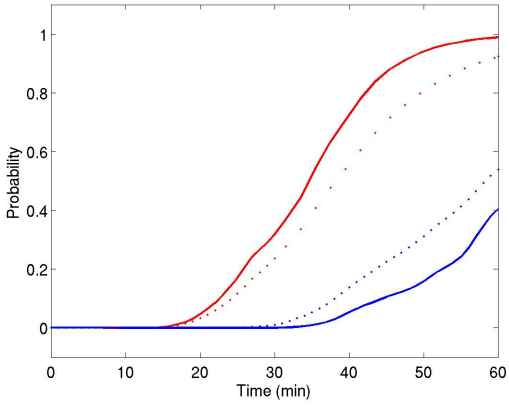

(f) Hall B1

Figure 3.13 *Probability of miosis in the public as a function of time after spill at pool 2. Red symbolizes LES, green and blue symbolizes RANS simulations on grid 1 and 2 respectively. The dotted lines indicate probabilities calculated from dose (P_D) and the full lines probabilities from toxic load (P_{TL}).*

4 Concluding remarks

Simulations of the dispersion of sarin through a convention centre have been conducted. The sarin vapour sources have been liquid pools at two different locations on the floor. Simulations with evaporation from each pool have been conducted separately. The dispersion of the resulting vapour has been simulated for an hour. From the resulting concentration fields possible timelines for the onset of various symptoms have been investigated.

A few simplifications and approximations were made for the simulations:

- One uncertainty is the evaporation model, which is developed for droplets or small pools, not for pools as big as in the current simulation. Furthermore the model includes two model variables which are parametrized for experimental measurements of a different substance, it could be that these could to some extent be specific to the chemical. However, the model should have a functional dependence on the friction velocity, and the resulting concentration fields should be scalable.
- Another simplification is that movement of people in the convention halls are disregarded. Since the velocities at ground level are very small, the air velocity caused by people moving might not be negligible. For the calculation of received doses, mean values in the various rooms are used and should diminish the error of neglecting the presence and movement of people somewhat. However, the movement of people might also lead to an increased evaporation rate, and thus larger concentrations of vapour in the rooms.
- The velocity inlets of the ventilation system are modelled as jets straight into the rooms. In reality, most ventilation systems have inlets which is directed outward as a cone, or with an obstruction impinging the air flow. However, it was concluded after a separate RANS simulation that this will not affect the evaporation rate, although it can have some effect on the subsequent dispersion of vapor.

Despite the above mentioned simplifications, the overall description of the dispersion and the following consequences are believed to be of importance for assessing the possible outcome and magnitude of a terror scenario with a chemical warfare agent.

The evaporation rate is very much dependent on the location of the pools due to differences in the local velocity field. In addition, there is a factor of 2-3 difference in the evaporation rate dependent on the CFD method; this is due to how different models calculate the velocity gradient near the surface, and thereby the friction velocity (which the evaporation model used depends on).

The onset of symptoms is investigated from the accumulated dose and the toxic load model. Near the pools, mild effects like miosis sets in within a few minutes, while severe effects or death do not occur until more than half an hour after the evaporation starts.

It is evident from the simulations that the vapour is not transported very efficiently away from the source. For pool 1, which is in a semi-confined room, is takes 10-30 minutes for the vapour to reach dangerous levels in the neighbouring rooms, by which time evacuation hopefully has at least started if not already taken place. For pool 2, which is in the hallway outside the rooms, very little vapour enters the rooms at all. Note however, that the evaporation rates in these cases are

quite low (order of milligrams per second). For substances with greater evaporation rates, the concentration levels will naturally be higher, but the relative concentration patterns should not be much affected (unless the concentration levels reaches high values and for instance dense gas effects become important).

The exfiltration rates from the outlets in the convention centre are monitored. Most of the vapour exits through the outlet in the part where the release source is located. A small amount of vapour is exfiltrated through the outlets in the corridor. The calculated exfiltration rates may be used as input for outdoor dispersion calculations to estimate the chemical threat to people outside the building.

Over all there is quite good agreement between the numerical approaches with respect to dispersion of the vapour and the consequence assessment. Due to the different evaporation rates obtained in with RANS and LES, the concentration levels differ somewhat, which again leads to differences in the onset of symptoms. Even though large eddy simulations give larger fluctuations in the velocity fields than Reynolds-averaged Navier-Stokes simulations, the standard deviations of the concentration fields are of the same sizes in the two methods. The obtained fluctuating concentration fields, with local maxima and minima of vapour concentration, could give different onset of symptoms than a more evenly distributed vapour concentration field. In the work at hand, however, spatial averages of the concentration fields are used for the consequence assessment.

The results from these high level dispersion calculations can be used for comparison with calculations with simpler and faster methods such as G-COMIS or CONTAM. The results can also be used for conducting exercises and for emergecy planning. A useful continuation of this work would be to conduct experiments, in order to validate the computational models.

A LES and RANS

A.1 Large Eddy Simulation

The spatial dimensions of the turbulent structures varies extensively. In LES, the large structures are computed explicitly, while the effect of structures smaller than a certain cut-off value are modelled. The small structures are thought to be fairly independent of the geometry for the flow (for instance the individual rooms in the present case), while the large structures are highly dependent on the geometry.

The velocity is filtered into the resolved and the sub-grid domain by equation A.1:

$$\overline{u_i} = \int G(x, x')u_i' dx' \tag{A.1}$$

Here, $\overline{u_i}$ is the filtered (resolved) velocity, and the filter function, $G(x, x')$ is usually related to the size of the computational cells. With the unfiltered velocity denoted by U_i the sub-grid velocity field is given by: $u_i = U_i - \overline{u_i}$. This results is the following equations:

$$\frac{\partial \overline{u_i}}{\partial t} + \overline{u_j}\frac{\partial \overline{u_i}}{\partial x_j} + \frac{\partial \tau_{ij}}{\partial x_j} = -1/\rho\frac{\partial \overline{p}}{\partial x_i} + \nu\frac{\partial^2 \overline{u_i}}{\partial x_j x_j} \tag{A.2}$$

$$\tau_{ij} = \overline{u_i u_j} - \overline{u}_i\overline{u}_j \tag{A.3}$$

where the bar denotes filtered parameters, $\nu = \mu/\rho$ is the kinematic viscosity, and τ_{ij} is the sub-grid scale stress tensor (which has to be modelled). For this work, the dynamic Smagorinsky-Lily subgrid scale model is used.

A.2 Reynolds Averaged Navier-Stokes

The RANS model is based on the Reynolds decomposition of the velocity field:

$$u_i = U_i + u_i' \tag{A.4}$$

where the instantaneous velocity, u_i, is decomposed in a mean velocity, U_i, and fluctuating velocity, u_i'. This results in the RANS equations:

$$\frac{\partial U_i}{\partial t} + U_j\frac{\partial U_i}{\partial x_j} = -1/\rho\frac{\partial P}{\partial x_i} + \nu\frac{\partial^2 U_i}{\partial x j^2} - \frac{\partial}{\partial x_j}\left(\overline{u_i' u_j'}\right) \tag{A.5}$$

$$\frac{\partial U_i}{\partial x_i} = 0 \tag{A.6}$$

where the last term in A.5 includes the Reynolds stress tensor, $\overline{u_i' u_j'}$. There are several models for this term, in this work the k-ϵ-model is used.

Bibliography

[1] Anthony T. Tu. *Chemical terrorism: Horrors in Tokyo Subway and Matsumoto City*. Alaken, Inc., Fort Collins, Colorado, 2002.

[2] Thor Gjesdal. *Oversikt over modeller for spredningssimulering*. FFI-notat 2003/00581, Forsvarets forskningsinstitutt, 2003.

[3] Monica Endregard, Bjørn Anders Pettersson Reif, Thomas Vik, and Odd Busmundrud. *Consequence assessment of indoor dispersion of sarin - A hypothetical scenario*. *Journal of Hazardous Materials*, 176:381–388, 2010.

[4] Pradyot Patnaik. *A comprehensive guide to the hazardous properties of chemical substances*. John Wiley & Sons, Inc., third edition, 2007.

[5] Emma Wingstedt, Bjørn Anders P. Reif, and Hannibal E. Fossum. *On a small scale aerosol release*. FFI-rapport 2012/00268, Forsvarets forskningsinstitutt, 2012. Distribution limited.

[6] ANSYS Fluent. web: http://www.ansys.com/Products/Fluids/ANSYS-Fluent.

[7] Stephen B. Pope. *Turbulent flows*. Cambridge university press, Cambridge, United Kingdom, 2000.

[8] Thomas Vik and Bjørn Anders Pettersson Reif. *Modeling the evaporation from a thin liquid surface beneath a turbulent boundary layer*. *International Journal of Thermal Sciences*, 50:2311–2317, 2011.

[9] Odd Busmundrud, Øyvind Voie, and Thomas Vik. *Effektmodellering ved eksponering for giftige kjemikalier - forklaring av "toxic load"*. FFI-rapport 2007/01140, Forsvarets forskningsinstitutt, 2007. In Norwegian.

[10] Jan H. Blanch and Åsmund Ukkelberg. CW database and prediction programs, 2001. CD published by FFI.

About FFI

The Norwegian Defence Research Establishment (FFI) was founded 11th of April 1946. It is organised as an administrative agency subordinate to the Ministry of Defence.

FFI's MISSION

FFI is the prime institution responsible for defence related research in Norway. Its principal mission is to carry out research and development to meet the requirements of the Armed Forces. FFI has the role of chief adviser to the political and military leadership. In particular, the institute shall focus on aspects of the development in science and technology that can influence our security policy or defence planning.

FFI's VISION

FFI turns knowledge and ideas into an efficient defence.

FFI's CHARACTERISTICS

Creative, daring, broad-minded and responsible.

Om FFI

Forsvarets forskningsinstitutt ble etablert 11. april 1946. Instituttet er organisert som et forvaltningsorgan med særskilte fullmakter underlagt Forsvarsdepartementet.

FFIs FORMÅL

Forsvarets forskningsinstitutt er Forsvarets sentrale forskningsinstitusjon og har som formål å drive forskning og utvikling for Forsvarets behov. Videre er FFI rådgiver overfor Forsvarets strategiske ledelse. Spesielt skal instituttet følge opp trekk ved vitenskapelig og militærteknisk utvikling som kan påvirke forutsetningene for sikkerhetspolitikken eller forsvarsplanleggingen.

FFIs VISJON

FFI gjør kunnskap og ideer til et effektivt forsvar.

FFIs VERDIER

Skapende, drivende, vidsynt og ansvarlig.

FFI's organisation

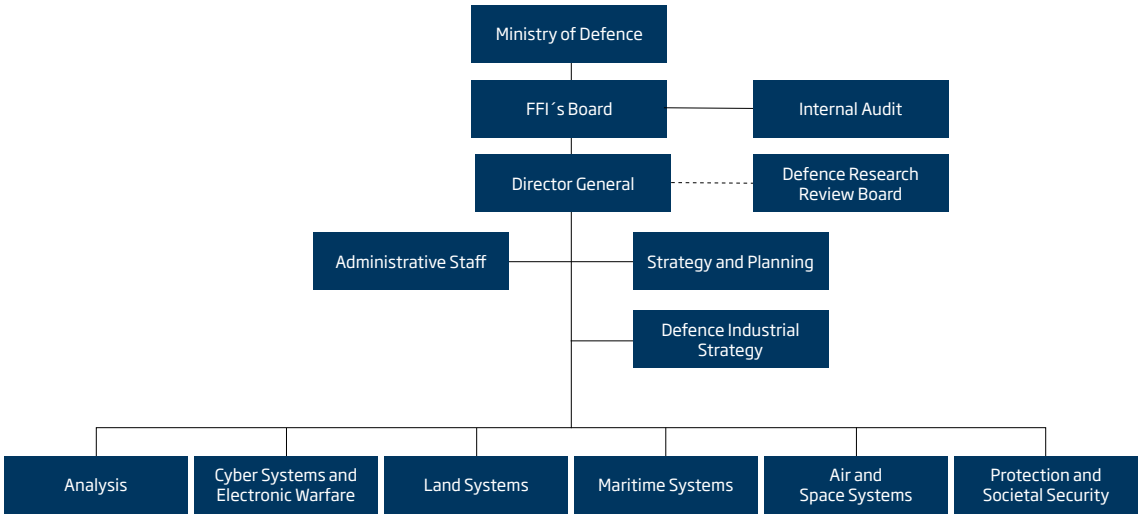

Forsvarets forskningsinstitutt
Postboks 25
2027 Kjeller

Besøksadresse:
Instituttveien 20
2007 Kjeller

Telefon: 63 80 70 00
Telefaks: 63 80 71 15
Epost: ffi@ffi.no

Norwegian Defence Research Establishment (FFI)
P.O. Box 25
NO-2027 Kjeller

Office address:
Instituttveien 20
N-2007 Kjeller

Telephone: +47 63 80 70 00
Telefax: +47 63 80 71 15
Email: ffi@ffi.no

FFI Forsvarets forskningsinstitutt
Norwegian Defence Research Establishment